Wind Power System Control Based on the Self-Synchronized Universal Droop Controller

Yang Ruan
Department of Electrical and Computer Engineering
Illinois Institute of Technology
Chicago, USA
yruan3@iit.edu

Qing-Chang Zhong, IEEE Fellow
Department of Electrical and Computer Engineering
Illinois Institute of Technology
Chicago, USA
zhongqc@ieee.org

***Abstract*—This paper presents a new control scheme for the back-to-back converter in a wind energy conversion system (WECS) that is equipped with a permanent magnetic synchronous generator (PMSG). The self-synchronized universal droop controller (SUDC) is utilized for both the rotor-side converter (RSC) and the grid-side converter (GSC). The DC-link voltage is regulated by the RSC instead of the GSC. The GSC is responsible for the maximum power point tracking (MPPT) and the grid integration. The control scheme does not involve the commonly-used abc/dq transformation, the phase-locked loop (PLL), or the motor encoder usually used in the field-oriented control to measure the rotor position/angle. The control scheme does not need the generator parameters either, therefore it is simple, and it is robust to system parameters. An experimental platform is built up to test the proposed control scheme and the results have demonstrated the effectiveness and good performance of the control scheme.**

***Index Terms*—wind energy conversion system (WECS), permanent magnetic synchronous generator (PMSG), self-synchronized universal droop controller (SUDC), back-to-back converter, maximum power point tracking (MPPT)**

I. Introduction

SUSTAINABLE energy penetration in power systems has been increasing for decades [1], due to governments' incentive policies to sustainable energies, technological development, as well as the cost reduction of products like solar panels, wind turbines, and generators. It has already become a trend for energy generation to shift from fossil fuels to sustainable resources, for which wind power plays a significant role.

The mainstream wind energy conversion systems (WECS) adopts variable-speed wind turbines because of the improved energy production and efficiency. The main topologies use either a double-fed induction generator (DFIG), or a permanent magnetic synchronous generator (PMSG). Compared to DFIG, PMSG is more likely to be used for direct-drive WECS where the gearbox and excitation system are removed. The direct-drive WECS is more simplified from the mechanical aspect, and it would be a better choice for the off-shore wind power plants due to the lower maintenance cost [2]. As shown in Fig. 1, PMSG is connected to the power grid with a fully rated back-to-back power converter.

This work was partially supported by the National Science Foundation under Grant No. 1810105.

A variety of control strategies have been developed for the back-to-back converter in wind power applications. Vector-oriented control is normally used for both the rotor-side converter (RSC) and the grid-side converter (GSC) [3], [4]. An encoder is usually mounted on the generator to measure the rotor position/angle. The rotor angle is thus used for the field-oriented control of the RSC. The controller of the GSC is normally oriented to the grid voltage vector, and a phase-locked loop (PLL) is required to synchronize the converter with the grid voltage. In some sensorless control strategies, the rotor angle and flux can be estimated so that the motor encoder is eliminated [5]–[7]. Vector control is usually implemented in the dq reference frame, where the direct and quadrature components are respectively regulated. Vector control strategies can be sensitive to parameters variations and mismatches, because decoupling terms related to the parameters are used to achieve desired field-orientation and generator parameters vary with different operating conditions. The synchronverter technology, which operates a power converter to mimic a synchronous machine [8], provides an alternative to control the back-to-back converter in wind power applications [9].

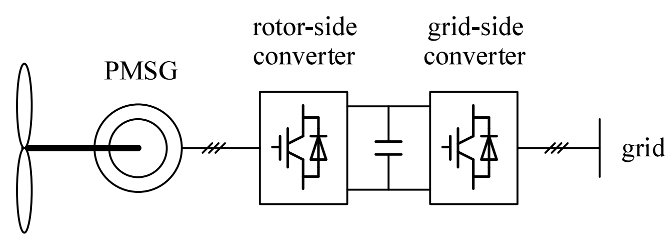

Fig. 1. Simplified schematic diagram of PMSG based wind energy conversion system.

In this paper, an original control scheme based on the recently proposed self-synchronized universal droop controller (SUDC) [10] is proposed for the back-to-back converter in a WECS equipped with a PMSG. The SUDC scheme is utilized to control both the rotor-side converter and the grid-side converter. The rotor-side converter works as a rectifier, maintaining the DC-link voltage to its reference value, and achieving the unity power factor operation. The grid-side converter is responsible for the maximum power point tracking (MPPT) and the grid integration. The proposed control scheme removes the motor encoder and the PLL and it is completely independent of PMSG parameters, which provides significant advantages on system performance. An experimental wind energy conversion system is built up to test the proposed control scheme with extensive experimental results presented to verify the proposed control scheme.

II. Overview of the Self-Synchronized Universal Droop Controller

The self-synchronized universal droop controller (SUDC) [10], as shown in Fig. 2, originates from the robust droop controller that achieves accurate power sharing for parallelly operated inverters with a resistive output impedance [11]. The robust droop controller is proven to be universal for any inverters having an output impedance angle between $-\frac{\pi}{2}$ to $\frac{\pi}{2}$ rad [12]. Furthermore, it is equipped with a self-synchronization mechanism so that it does not need a PLL.

The SUDC has different operation modes, as summarized in Table I, by controlling switches S_P, S_Q, and S_C. Each operation mode achieves an unique function. In this paper, the self-synchronization mode and power set mode ($P-$mode, $Q-$mode) are utilized for wind power applications, which will be discussed in this section. More details on the droop mode, i.e., the P_D-mode, Q_D-mode , can be found in [10], [11].

TABLE I
Operation modes of the SUDC

Mode	Switch S_C	Switch S_P	Switch S_Q
Self-synchronization mode	s	OFF	OFF
P-mode, Q-mode	g	OFF	OFF
P_D-mode, Q-mode	g	ON	OFF
P-mode, Q_D-mode	g	OFF	ON
P_D-mode, Q_D-mode	g	ON	ON

A. Self-synchronization mode

As shown in Fig. 2, the SUDC involves two channels. One channel to regulate the real power, and the other to regulate the reactive power. To enable the self-synchronization mode, both the switch S_P and the switch S_Q are turned OFF with the switch S_C set at position s. Setting $i = i_s$ and both P_{set} and Q_{set} to zero, the SUDC satisfies

$$\dot{E} = n(P_{set} - P) \quad (1)$$

$$\omega = \omega^* - \frac{mK}{s}(Q_{set} - Q) - m(Q_{set} - Q) \quad (2)$$

When the virtual current i_s is regulated to zero, the terminal voltage v_o is the same as the grid voltage v_g. In other words, the terminal voltage v_o of the inverter is synchronized with the grid voltage v_g. After the synchronization is achieved, the relay in the inverter can be turned ON to connect the inverter to the grid. At the same time, the switch S_C should be turned to position g so that the real grid current i_g can be fed into the SUDC for the power calculation.

B. Set mode ($P-$mode and $Q-$mode)

For the set mode, either the real power or the reactive power are regulated to the reference values. To enable the $P-$mode, the switch S_P is turned OFF, and the real power channel of the SUDC satisfies

$$\dot{E} = n(P_{set} - P)$$

The voltage magnitude E settles down at a constant value in the steady state, which results in

$$P = P_{set}$$

Thus the real power P_{set} is sent to the grid. Similarly, the $Q-$mode is enabled by switching S_Q to OFF, and the reactive power channel satisfies

$$\omega = \omega^* - \frac{mK}{s}(Q_{set} - Q) - m(Q_{set} - Q)$$

The frequency settles down in the steady state, which results in

$$Q = Q_{set}$$

Thus the desired reactive power Q_{set} is sent to the grid.

In the following sections, the SUDC is utilized to control the back-to-back converter for a wind energy conversion system equipped with a PMSG.

III. Control of the Rotor-Side Converter

In this paper, the main task of the rotor-side converter is to maintain a constant DC-link voltage, thus the converter works as a PWM-rectifier. Fig. 3 shows the control scheme for the rotor-side converter. Several changes are made in Fig. 3 compared to the SUDC shown in Fig. 2. (1) The switch S_P and the term $K_e(E^* - V_o)$ are eliminated, which means the real power droop mode P_D is disabled, and the real power set mode ($P-$mode) is enabled. (2) A DC-link voltage controller is added to generate the real power reference P_{rset}. In this way, the real power flows into the converter from the generator, through which the DC-link voltage is maintained. (3) A proportional integral controller ($k_{pQr} + \frac{k_{iQr}}{s}$) replaces the integration term $\frac{K}{s}$, which speeds up the reactive power regulation.

It is also clear that the real power and the reactive power are separately regulated. The real power channel has two cascaded control loops. The inner loop is the real power control loop with the feedback coming from real power calculation via the generator voltage v_r and the current i_{or} and the outer loop is the DC-link voltage control loop with the feedback directly coming from the measured DC-link voltage U_{dc}. The reactive power Q of the rotor-side converter is controlled to track the reference Q_{rset}. Due to the PI controller ($k_{pQr} + \frac{k_{iQr}}{s}$) in the reactive power channel, the reactive power will be the same as the reference value in the steady state. For the wind power application in this paper, the reactive power reference Q_{rset} is set as zero to achieve unity power factor operation.

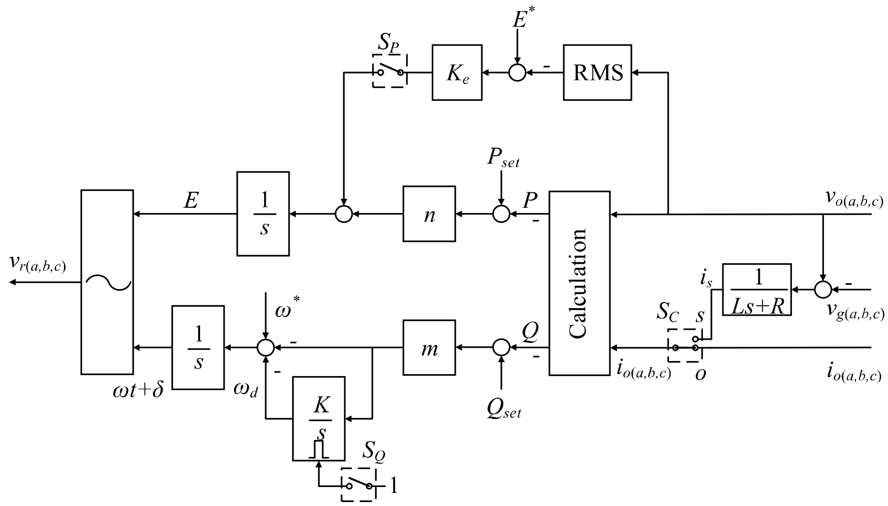

Fig. 2. Self-synchronized universal droop controller.

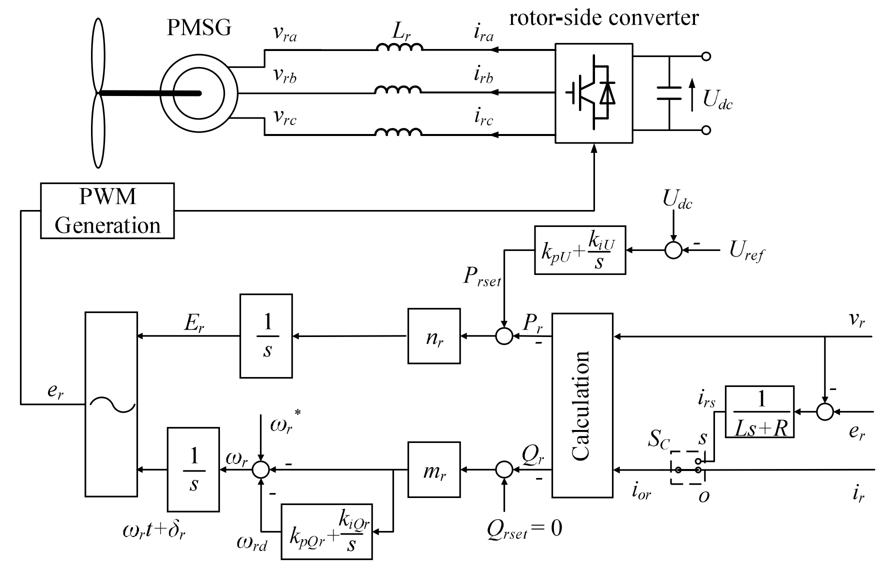

Fig. 3. Control scheme for the rotor-side converter.

IV. Control of the Grid-Side Converter

The grid-side converter is used for grid integration as well as extracting the maximum power from the wind. The high efficiency of the variable speed wind energy conversion system is basically achieved by MPPT control algorithms. Wind power curves can be used to extract the maximum power from the wind turbine under all operating conditions. The wind turbine can be regulated to its maximum power operating points for various wind speeds by maintaining the tip speed ratio to the value that maximizes its aerodynamic efficiency.

For a variable speed wind turbine, the wind power that can be captured by the blades and then converted to mechanical power is

$$P_M = \frac{1}{2}\rho\pi R^2 v_w^3 C_p, \tag{3}$$

where P_M is a cubic function of the wind speed v_w, ρ is the air density, r_T is the turbine radius and $C_p = f(\lambda, \beta)$ is the power coefficient, which depends on the tip speed ratio λ of the wind turbine and the blades angle β. The tip speed ratio is defined as

$$\lambda = \frac{\omega_n r_T}{v_w} \tag{4}$$

where ω_n is the rotor speed of wind turbine.

When the wind speed is lower than the rated speed, in order to capture the maximum power from wind, the rotor speed should be regulated to achieve the optimal tip speed ratio λ_{opt}. Generally λ_{opt} is a constant value for a certain turbine, therefore the power coefficient C_p becomes a constant value $C_{p,opt}$ when λ_{opt} is achieved. According to (3)-(4), the maxmum mechanical power can be rewritten as

$$P_{M,max} = K_{opt}\omega_n^3 \tag{5}$$

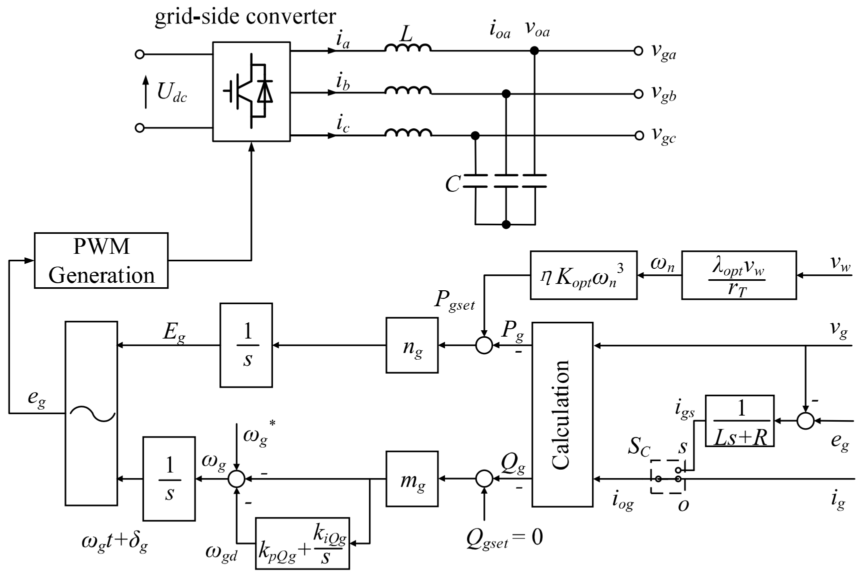

Fig. 4. Control scheme for the grid-side converter.

where

$$K_{opt} = \frac{\rho\pi R^5 C_{p,opt}}{2\lambda_{opt}^3} \tag{6}$$

and

$$\omega_n = \frac{\lambda_{opt} v_w}{r_T}. \tag{7}$$

Following the SUDC strategy, the control scheme for the grid-side converter is shown as in Fig. 4. Similar to the controller of the RSC, both the $P-$mode and $Q-$mode of the SUDC are utilized, and the real power and the reactive power are separately regulated. For the reactive power channel, Q_{gset} is set as zero to achieve unity power factor operation. To track the maximum power point, the target rotor speed ω_n is firstly calculated according to the optimal tip speed ratio λ_{opt} and the wind speed v_w, and then the real power reference P_{gset} for the GSC is calculated as

$$P_{gset} = \eta K_{opt}\omega_n^3 \tag{8}$$

Taking into account the power losses of the whole system, the coefficient η is less than 1.0 to make sure that the real power reference P_{gset} is smaller than the maximum mechanical power $P_{M,max}$. The coefficient may be changed for different systems, and it could be estimated by the power level of the back-to-back converter and PMSG within a wide range of operating conditions.

V. Experimental results

An experimental platform for the wind energy conversion system is built up to test the proposed control schemes. The experimental platform is shown in Fig. 5. A synchronous generator with a fixed field works as a permanent magnetic synchronous generator. The synchronous generator is integrated to the power grid via a three-phase back-to-back converter. The wind turbine is simulated by an induction motor driven by a three-phase inverter. Since only the single-phase power grid is available in the lab, a single-phase input three-phase output power converter is developed to work as the power grid for the experiments.

TABLE II
Parameters of the synchronous generator

Parameters	Values
Rated generator output power	200 VA
State voltage (phase voltage)	120 V
Rated speed	1800 rpm
Stator resistance	12.5 Ω
Rotor resistance	125 Ω
Stator leakage reactance	18.6 Ω
d-axis transient reactance x_d'	31.5 Ω
q-axis transient reactance x_q'	123 Ω
Pole pairs	2

The wind profile is programmed/loaded into the motor driver, where the motor speed is regulated via the wind speed and the optimal tip speed ratio λ_{opt}. The back-to-back converter is controlled by the above-mentioned controllers. In this way, the wind energy conversion system regulates the output power according to the wind speed via changing the rotor speed to reach the optimal tip speed ratio λ_{opt}, therefore achieving the MPPT function.

The switching frequency for the back-to-back converter is 16kHz, and the sampling frequency is 5.33kHz. Other parameters of the system are listed in Table II.

The system is operated in the following sequence:

(1) Start the three-phase inverter to drive the induction motor that works like a wind turbine and control the motor speed to the initial speed of 1500 rpm. The synchronous generator works simultaneously with voltage generated.

(2) Start the rotor-side converter, and regulate the DC-link voltage to 400 V with the reactive power reference set at zero, i.e., Q_{rset}= 0.

(3) Start the grid-side converter with both the real and reactive power references set as zero, i.e., P_{gset}= 0, and Q_{gset}= 0 and then connect it to the grid after synchronization. The entire system works with zero power transmitted to the grid.

(4) Set the active power reference for the grid-side converter as $P_{gset} = 0.75K_{opt}\omega_n^3$, therefore the desired real power transfers from the PMSG to the grid. Consider the test time as $t = 0$ from now on.

(5) Change the rotor speed according to a wind profile. The wind profile consists of five parts. 1) for the first 8 seconds, the rotor speed is regulated as 1500 rpm; 2) at $t = 8$ s, the rotor speed increases to the rated speed (1800 rpm) within 1 second, and then remains at 1800 rpm for 7 seconds; 3) at $t = 16$ s, the rotor speed decreases to 1650 rpm within 1 second, and then remains at this speed for 7 seconds; 4) from $t = 24$ s, the speed follows a two-period sinusoidal curve, where the frequency is 0.25 Hz, and the amplitude is 150 rpm; 5) at $t = 32$ s, the speed comes back to 1650 rpm and lasts for 8 seconds.

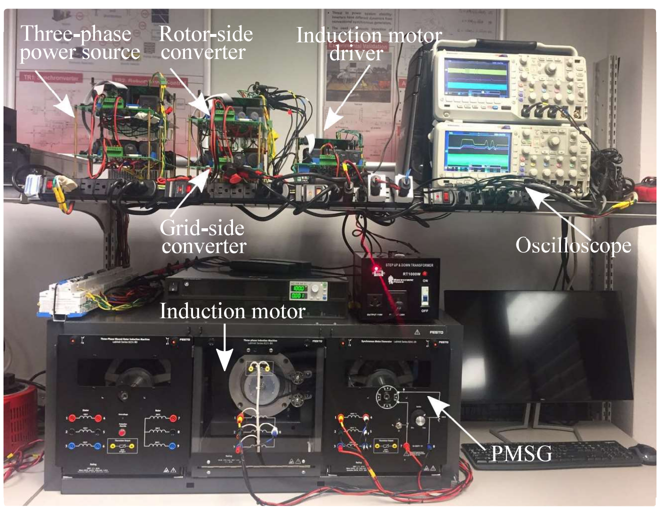

Fig. 5. Experimental platform for the PMSG wind energy conversion system

A. Rotor-side converter performance

Dynamic responses of the rotor-side converter are shown in Fig. 6 to Fig. 7. Fig. 6(a) shows the dynamic responses of the rotor speed of the synchronous generator, and the DC-link voltage. It is clear that the DC-link voltage is regulated to its reference value 400V satisfactorily. The DC-link voltage varies with respect to the rotor speed, and there is nearly 20 volts ripple during rotor speed variation. Fig. 6(b) shows the dynamic responses of the real power and reactive power that are extracted from the synchronous generator. The upper line is the real power which changes with respect to the rotor speed. The bottom plot shows the reactive power which is stabilized to zero quickly after the rotor speed changes. Fig. 6(c) shows the voltage and current of the synchronous generator. Fig. 7

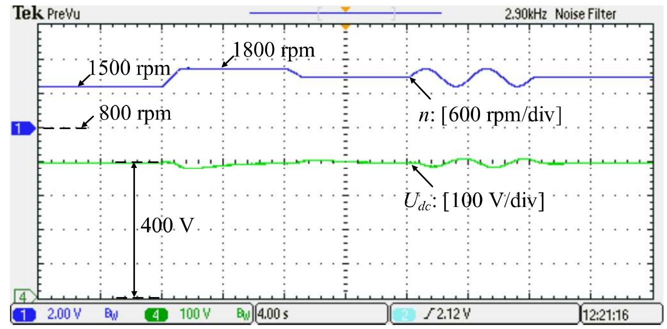

(a)

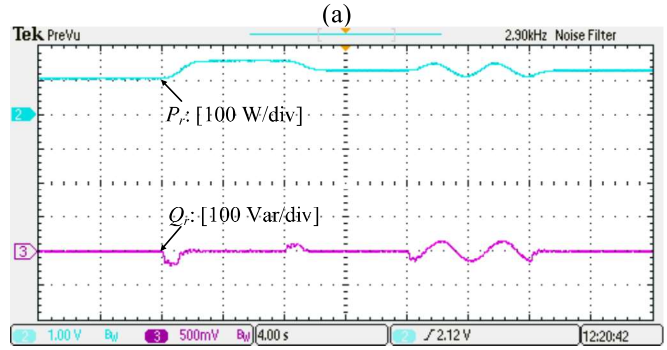

(b)

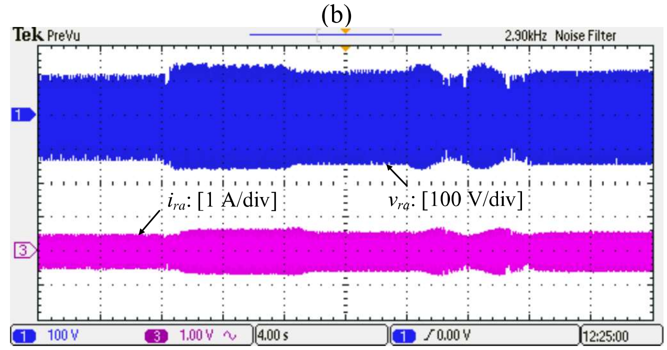

(c)

Fig. 6. Dynamic response of the rotor-side converter: (a) rotor speed and DC-link voltage, (b) real power and reactive power, (c) PMSG generator voltage and current.

shows the generator voltage and current when the wind speed is changed from 1800 rpm to 1650 rpm. The generator current is in phase with the voltage, which achieves unity power factor operation.

B. Grid-side converter performance

Fig. 8(a) shows the responses of the real power and reactive power that are injected to the grid. Fig. 8(b) shows the voltage and current curves of the grid-side converter. The real power curve in Fig 8(a) is smooth and stable with respect to the change of the rotor speed, and it can track the maximum power from the wind turbine. The reactive power plot in Fig 8(b) is aligned with the expectation of Q-mode operation and it is regulated to zero without ripple.

VI. Conclusions

A strategy to control the back-to-back converter in a variable-speed wind energy conversion system equipped with

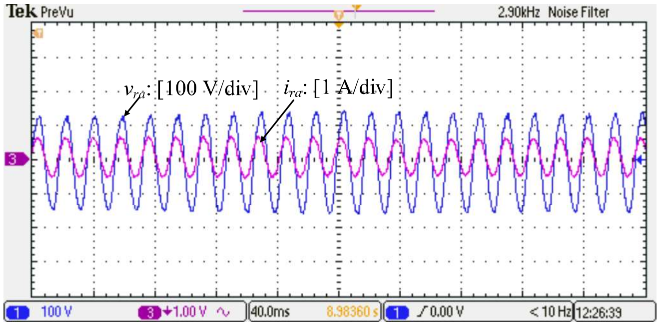

Fig. 7. PMSG generator voltage and current when the wind is changed from 1800 rpm to 1650 rpm.

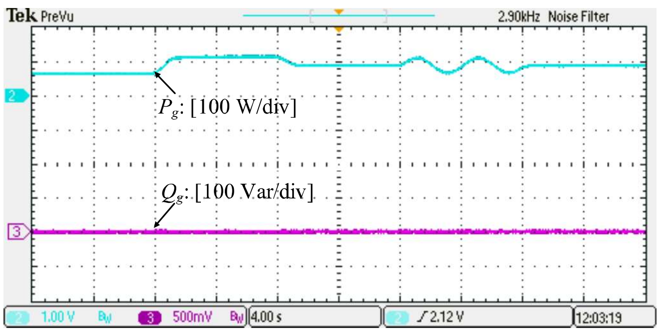

(a)

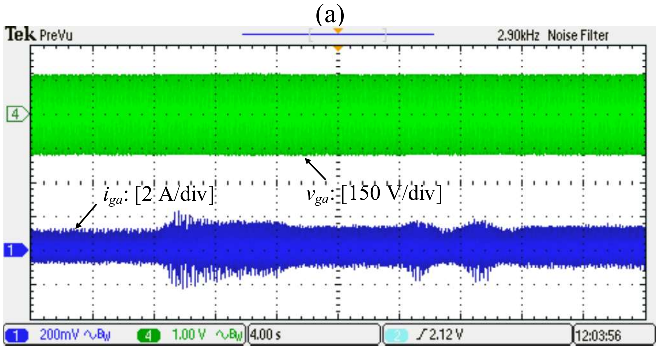

(b)

Fig. 8. Dynamic response of the grid side converter: (a) real power and reactive power, (b) voltage and current.

a permanent magnetic synchronous generator is proposed, via adopting the self-synchronized universal droop controller for both the rotor-side converter and the grid-side converter. The rotor-side converter regulates the DC-link voltage to its reference value, while the grid-side converter is responsible for the MPPT function and the grid integration. The commonly-needed PLL and motor encoder are removed. The proposed control strategy is simpler compared to the field-oriented control and it is completely independent of the generator parameters. It not only decreases the calculation burden of digital signal processors (DSP) but also guarantees the robustness of the controllers. An experimental platform for a wind energy conversion system is built up to test the proposed method and experimental results have verified the good performance of the controllers.

REFERENCES

[1] V. Yaramasu, B. Wu, P. C. Sen, S. Kouro, and M. Narimani, “High-power wind energy conversion systems: State-of-the-art and emerging technologies,” *Proc. IEEE*, vol. 103, no. 5, pp. 740–788, May 2015.

[2] V. Yaramasu, A. Dekka, M. J. Duran, S. Kouro, and B. Wu, “Pmsg-based wind energy conversion systems: survey on power converters and controls,” *IET Electric Power Appli.*, vol. 11, no. 6, pp. 956–968, 2017.

[3] Z. Zhang, Y. Zhao, W. Qiao, and L. Qu, “A discrete-time direct torque control for direct-drive pmsg-based wind energy conversion systems,” *IEEE Trans. Ind. Electron.*, vol. 51, no. 4, pp. 3504–3514, July 2015.

[4] R. Errouissi, A. Al-Durra, and M. Debouza, “A novel design of pi current controller for pmsg-based wind turbine considering transient performance specifications and control saturation,” *IEEE Trans. Ind. Electron.*, vol. 65, no. 11, pp. 8624–8634, Nov 2018.

[5] Z. Zhang, Y. Zhao, W. Qiao, and L. Qu, “A space-vector-modulated sensorless direct-torque control for direct-drive pmsg wind turbines,” *IEEE Trans. Ind. Electron.*, vol. 50, no. 4, pp. 2331–2341, July 2014.

[6] M. Benadja and A. Chandra, “Adaptive sensorless control of pmsgs-based offshore wind farm and vsc-hvdc stations,” *IEEE J. Emerg. Sel. Topics Power Electron.*, vol. 3, no. 4, pp. 918–931, Dec 2015.

[7] R. I. Putri, M. Pujiantara, A. Priyadi, T. Ise, and M. H. Purnomo, “Maximum power extraction improvement using sensorless controller based on adaptive perturb and observe algorithm for pmsg wind turbine application,” *IET Electric Power Appli.*, vol. 12, no. 4, pp. 455–462, 2018.

[8] Q.-C. Zhong and G. Weiss, “Synchronverters: Inverters that mimic synchronous generators,” *IEEE Trans. Ind. Electron.*, vol. 58, no. 4, pp. 1259–1267, April 2011.

[9] Q.-C. Zhong, Z. Ma, W.-L. Ming, and G. Konstantopoulos, “Grid-friendly wind power systems based on the synchronverter technology,” *Energy Conversion and Management*, vol. 89, 01 2015.

[10] Q.-C. Zhong, W. Ming, and Y. Zeng, “Self-synchronized universal droop controller,” *IEEE Access*, vol. 4, pp. 7145–7153, 2016.

[11] Q.-C. Zhong, “Robust droop controller for accurate proportional load sharing among inverters operated in parallel,” *IEEE Trans. Ind. Electron.*, vol. 60, no. 4, pp. 1281–1290, April 2013.

[12] Q.-C. Zhong and Y. Zeng, “Universal droop control of inverters with different types of output impedance,” *IEEE Access*, vol. 4, pp. 702–712, 2016.